

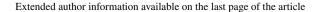
Solute–Solvent Interactions of 2,2,6,6-Tetramethylpiperidinyloxyl and 5-Tert-Butylisophthalic Acid in Polyethylene Glycol as Observed by Measurements of Density, Viscosity, and Self-Diffusion Coefficient

Markus M. Hoffmann¹ · Nathaniel P. Randall¹ · Miray H. Apak¹ · Nathaniel A. Paddock¹ · Torsten Gutmann² · Gerd Buntkowsky²

Received: 6 December 2022 / Accepted: 10 February 2023 / Published online: 21 March 2023 © The Author(s), under exclusive licence to Springer Science+Business Media, LLC, part of Springer Nature 2023

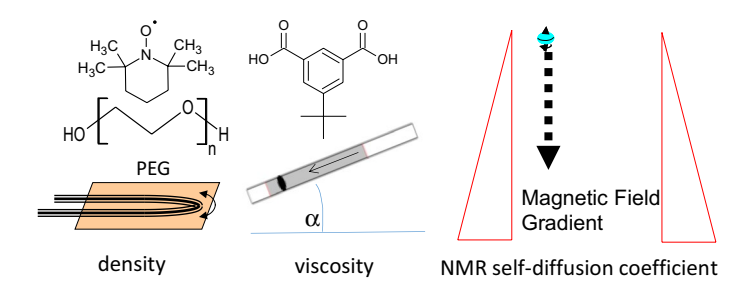
Abstract

This study is seeking a better understanding of polyethylene glycol (PEG) as a solvent to promote its use in chemical synthesis. The effect of adding two solutes of interest, 2,2,6,6-tetramethylpiperidinyloxyl (TEMPO) and 5-tert-butylisophthalic acid (5-TBIPA) to PEG200 (average molar weight of 200 g·mol⁻¹) on the solution density, viscosity, and selfdiffusion coefficients is monitored in a temperature range of 298.15-358.15 K to deduce how these solutes interact with the PEG200 solvent. The effect of water, the most common impurity in PEGs, is also monitored and found to be nearly negligibly small. Addition of (5-TBIPA) increases solution density and viscosity. Combined with the observation that 5-TBIPA consistently self-diffuses at about half the rate as PEG200 at all investigated experimental conditions, this suggests strong attractive solute-solvent interactions likely through hydrogen bonding interactions. In contrast, addition of TEMPO causes lower solution densities and viscosities suggesting that the solute-solvent interactions of TEMPO lead to an overall weakening of the intermolecular interactions present compared to neat PEG200. Inspection of the viscosity and self-diffusion temperature dependence reveals slight deviations from the Arrhenius equation. Interestingly, the activation energies obtained from the viscosity and the self-diffusion data are essentially identical in values suggesting that the same dynamic processes and thus the same activation barriers govern translational motion and momentum transfer in these PEG200 solutions.





Graphical Abstract



Keywords Polyethylene glycol · Self-diffusion · Viscosity · Density · 2,2,6,6-Tetramethylpiperidinyloxyl · 5-Tert-butylisophthalic acid

1 Introduction

Polyethylene glycol (PEG, H–[O–CH₂–CH₂]_n–OH) has experienced increased interest as an alternative solvent for chemical synthesis, which several recent review articles on this subject demonstrate [1–3]. PEG is widely and relatively inexpensively available because it is an industrial commodity with an annual production of about 500,000 tons per year [4] mainly for the personal and healthcare industries [5–7]. PEG is commercially available as polydisperse mixtures. The product name indicates the average molar weight. Lower molar weight PEGs such as PEG200, where the average molar weight is approximately 200 g·mol⁻¹, are liquid at ambient conditions.

Several properties of lower molar weight PEGs are very favorable compared to traditional organic solvents. PEGs are non-toxic, possess a low vapor pressure, which reduces exposure through inhalation, and they are biodegradable [8]. Lower molar weight PEGs can dissolve a wide range of chemicals including some mineral salts [9], which allow them to be advantageously used as a medium for making metal organic frameworks (MOFs) [10, 11]. A physicochemical understanding of PEGs as a solvent would be desirable to aid the continuing research efforts of using PEGs as a medium for chemical synthesis. As recently reviewed [12], relevant physicochemical studies are unfortunately very limited. Therefore, our laboratory has recently focused on the physical properties density, viscosity, and selfdiffusion coefficient [13, 14] to investigate the effect of water and PEG200 composition (vendor source) on these properties and how generally these properties can be derived from knowledge of PEG composition and the properties of the neat ethylene glycol oligomer components. It was found that these three physical properties show only very small, if any, dependence on both water content up to about 0.15 mol fractions and mixture composition. Volumetric properties displayed ideal mixing behavior, and even the viscosities and self-diffusion coefficients of PEG200 (as well as a binary mixture of tri- and hexaethylene glycol) could be reasonably well obtained from summation of the mole fraction weighted property contribution of each neat oligomer. This study is a continuation of these efforts where the effect of a couple of different solutes on these properties was investigated. The solutes chosen were 2,2,6,6-tetramethylpiperidinyloxyl (TEMPO) and 5-tert-butylisophthalic acid (5-TBIPA). Their chemical structures are shown in Scheme 1. TEMPO is a stable free radical important in chemical transformations [15], in particular as redox catalyst



Scheme 1 Chemical structure of 2,2,6,6-Tetramethylpiperidinyloxyl (TEMPO) and 5-tert-butylisophthalic acid (5-TBIPA)

[16]. TEMPO has also been frequently used as a spin probe [17] and spin label [18] for the study of intermolecular interactions and elucidation of structural details. TEMPO was also chosen for this study to aid the increasing research area of dynamic nuclear polarization (DNP) in NMR spectroscopy where the presence of a compound with unpaired electrons as polarization agent is required, and many polarization agents are based on TEMPO as the free radical moiety [19–25]. 5-TBIPA was chosen because it is one possible reagent to form MOFs [11]. 5-TBIPA is somewhat larger in size as TEMPO and possesses different functional groups. Both compounds are sufficiently soluble in PEG200 to allow for solute concentration-dependent measurements.

Physical property studies of binary systems involving PEG200 have been reported in the literature. These all involved a second liquid (solvent) that is completely miscible with PEG200. Most of these studies measured density to obtain excess molar volumes [26–43]. In a similar vein, many of these and other reports investigated additional physical properties including viscosity [27, 30–32, 34–37, 39–41, 44–46], index of refraction [26, 27, 29–39, 41–47], relative permittivity [38, 44, 45], enthalpy of mixing [27], heat capacity [36], and speed of sound [29, 37, 43]. We are only aware of one study focusing on PEG200 solutions with dissolved solid solutes, namely a refractometric study of polymers in PEG200 [48]. Furthermore, to the best of our knowledge, this is the first investigation of self-diffusion in PEG200 solutions.

As for the organization of the remainder of this report, after providing experimental details in Sect. 2, the results are presented and discussed in Sect. 3 focusing first on the water dependence of the physical properties, next their temperature dependence, and finally their solute concentration dependence. Section 3 finishes with a molecular level interpretation of the results with emphasis on hydrogen bonding interactions. Section 4 summarizes the main conclusions of this study.

2 Experimental

2.1 Preparation of Samples

All chemicals with specifications as summarized in Table 1 were used as received. We note that PEG vendors typically do not state the mass fraction purity possibly because PEGs are polydisperse mixtures, and we assume that the mass fraction purity is of typical value of 0.99. The exact composition of PEG200 has been analyzed in previous work and for convenience is tabulated in Table S1 [14]. Two TEMPO sources were used for measurements to test reproducibility of results. The PEG and solute components were stored and mixed



Chemical name	CAS	Source	Mass fraction purity ^a
PEG200	25322-68-3	Acros	Not specified ^b
5-tert-Butylisophthalic acid	2359-09-3	Sigma Aldrich	0.98
2,2,6,6-Tetramethylpiperidinyloxyl	2564-83-2	MP Biochemicals	0.98
2,2,6,6-Tetramethylpiperidinyloxyl	2564-83-2	AA Blocks	0.97
Water	7732-18-5	Anton Paar	"Ultra-pure"

Table 1 Information on chemicals used

under inert atmosphere in a glove box and if needed stirred until complete dissolution was achieved. We intended to study concentrations up to 0.3 molar to cover typical concentrations of polarizing agents in DNP-enhanced NMR spectroscopy. We found that the solubility limit of 5-TBIPA in PEG200 is below 0.3 mol·l⁻¹, and thus, data for PEG200 solutions with 5-TBIPA could only be acquired up to 0.15 mol·l⁻¹. Addition of water was done outside of the glovebox, after which the sample was vigorously shaken for several minutes. The water content of each prepared sample was measured at least trifold after completion of density and viscosity measurements using a fritless C20 Mettler Toledo Karl Fischer (KF) with a relative standard deviation (RSD) of generally 0.1. A 5-ml plastic syringe was used for injection of solution into the combined density meter and viscometer. Samples for NMR measurements were placed in a 5-mm NMR tube (standard tube or with valve), and a flame-sealed capillary with D₂O as lock solvent was added before the NMR tube was either flame sealed or sealed using a closed valve.

2.2 Density and Viscosity Measurements

Densities and viscosities were measured in parallel with, respectively, an Anton Paar DMA 4100 M vibrating tube density meter with internal correction of sample viscosity effects and an Anton Paar Lovis 2000 M/ME rolling ball viscometer using a 1.8 mm capillary. Both instruments are temperature controlled by Peltier systems with stated accuracy of 0.02 K. Samples were measured in a temperature series from 298.15 to 358.15 K in 10 K increments and then back to 298.15 K to check that initial and final 298.15 K results agreed with each other. The averages of at least six repeat measurements are reported. The proper calibration of both instruments was tested by repeating measurements with neat PEG200 that were recently reported [14]. Results agreed within 0.5 mPa·s for the viscosity measurements and within 0.1 kg·m⁻³ for the density measurements.

2.3 Self-Diffusion Coefficient Measurements

All NMR data were acquired on a Bruker Avance 300 NMR spectrometer with a variable temperature broadband probe. Each sample was allowed to temperature equilibrate for at least 20 min. The sample NMR tube was not spun during temperature equilibration and data acquisition. The actual sample temperature was determined at the beginning and the end of a measurement series consisting of typically 6–12 samples at constant temperature using a neat ethylene glycol sample for which the dependence



^aAs stated by vendor

^bPresumably not specified because PEGs are polydisperse

of the chemical shift on temperature is known [49]. From these ethylene glycol measurements, an estimate of 0.5 K is obtained as the standard temperature uncertainty. A double stimulated echo pulse sequence [50, 51] was used to obtain self-diffusion coefficients. The pulse sequence includes bipolar gradients and three spoiler gradients with 5 ms eddy current recovery and 0.2 ms gradient recovery. The recycling delays were set to at least three times the spin lattice (T_1) relaxation time. The field gradient strength was linearly increased from 0.543 to 54.3 G·mm⁻¹ to obtain a total of 16 different gradient strengths. The number of repetition scans was set to 16 and the number of dummy scans to 4. To obtain the self-diffusion coefficients, the stimulated spin-echo intensity, I(g), of each proton signal was fit to Eq. 1, with the magnetic field gradient strength, g, as the independent variable [52]

$$I(g) = I_0 e^{-D\gamma^2 g^2 \delta^2 \left((4\Delta - \delta)/\pi^2 \right)} \tag{1}$$

where I_0 is the reference spin-echo intensity in the absence of gradient, γ is the ¹H gyromagnetic ratio (=2.6752218744×10⁸·s⁻¹·T⁻¹), Δ is the diffusion time (=0.1 s), and δ is the length of the sine-shaped gradient pulse that depends on the sample and temperature condition. Based on the experiences from prior studies [13, 14, 53], the standard uncertainty of the self-diffusion coefficients is 0.1×10^{-10} m²·s⁻¹, which is about as much as the lowest measured self-diffusion coefficients reported for the lowest temperature of 298.15 K. We caution that the standard uncertainty might be higher for the PEG200 selfdiffusion coefficients from the TEMPO solutions. Signals from the free radical compound TEMPO in solution of PEG200 are unobservable in the ¹H NMR spectrum because its unpaired electron spoils the local magnetic field around TEMPO, which broadens the ¹H NMR signals of TEMPO so much that they disappear in the base line. With increasing TEMPO concentration, line broadening is observed for the PEG200 ¹H NMR signals leading to severe overlap of PEG200 signals. Moreover, the spoiled local magnetic fields also become spin-lattice (T₁) relaxation sinks. At TEMPO concentrations larger than 0.02 molar, T₁ relaxation times were observed to be on the order of milliseconds, which is too fast for measuring self-diffusion coefficients with the pulsed-field gradient method employed in this study. Thus, only the self-diffusion coefficients of PEG200 are reported for the TEMPO solutions and only to maximal 0.02 molar concentrations.

5-TBIPA is not a free radical compound, and no such concerns as just described apply for measuring the self-diffusion coefficient of the 5-TBIPA solute and the PEG200 solvent. 5-TBIPA affords multiple signals in the ¹H NMR spectrum from the aromatic rings in addition to the strong line of the tert-butyl functional group. The reported 5-TBIPA self-diffusion coefficients represent the average values obtained from these signals. Although the PEG200 ¹H NMR spectrum displays three proton signals, one signal for the hydroxy protons, one signal for the CH₂ protons next to ether oxygens ("CH₂-O"), and one signal for the CH₂ protons next to the hydroxy end group ("CH₂-OH"), the self-diffusion coefficient of PEG200 cannot be taken as the average of these three signals. Instead, the PEG200 self-diffusion coefficient should be taken from the CH₂OH signal alone [14] as it represents the mole fraction averaged self-diffusion coefficient of the polydisperse ethylene glycol mixture of PEG200 while using the CH₂-O signal would lead to artificially slower self-diffusion coefficients because the weighting of each ethylene glycol oligomer increases with its number of ether oxygens. The signal of the hydroxy protons is not usable because of chemical proton exchange with water protons, hence the label of "OH/H₂O" in this work.



3 Results and Discussion

3.1 Water Content Dependence and Data Quality

Water is a primary impurity of PEGs because it can readily absorb water from the atmosphere. Prior studies showed that the water content up to mass fractions of about 0.02 hardly changes density, viscosity, and self-diffusion of PEG200, and the neat "dry" PEG property values were obtained by linear extrapolation to zero water content [14]. Anticipating similar behavior in this study for various PEG200 solutions, the property measurements were obtained in this study from only two sets of samples, one set without and one set with small amounts of added water. Figure 1 shows one illustrative set of density data for the case of solutions of TEMPO (from MP Biochemicals) in PEG200 at room temperature. These and the remaining density data sets are tabulated in Tables S2-S4 in the supplementary materials. Figure 1 shows that the addition of water systematically leads to slightly smaller densities. The densities of the "dry" PEG200 solutions, summarized in Table 2, were obtained by linear extrapolation to zero water content. They are generally only by about 0.1 kg·m⁻³ higher than the corresponding densities of the samples containing water at about 0.002 mass fraction of water. The addition of water also generally lowers the viscosity as can be seen from the data sets summarized in Tables S5-S7 in the supplementary materials. However, there is more random error in the viscosity data sets such that there are in Tables S5 and S7 a few instances marked with red coloring where the viscosity either slightly increases or decreases too steeply. This is illustrated in Fig. 2 for the case of TEMPO solutions at 298.15 K that includes one instance where the viscosity increases with water addition (added cross in square symbols) and one instance where the viscosity obtained after water addition appears to fall too steeply (added plus in diamond symbols). Water addition should decrease not increase the viscosity, and for most of the entries in Tables S5, S6, this decrease is very small, 0.3 mPa·s or less. Therefore, as criterion for "too steeply" we took that either the slope value was at least an order of magnitude larger than generally observed at a given temperature or the "intercept" differed by more than 1 mPa·s from the viscosity obtained from the sample with ~0.002 mass fraction of water present. In these cases, an average slope value obtained from the other concentration data at same temperature was used to extrapolate to zero water mass fraction. In the case of positive slopes,

Fig. 1 Densities of solutions of TEMPO in PEG200 as a function of water mass fraction of present water at TEMPO concentrations 0.0106 (squares), 0.0191 (circles), 0.0399 (diamonds), 0.0761 (down triangles), 0.1460 (up triangles), and 0.2872 (left triangle) mol·l⁻¹

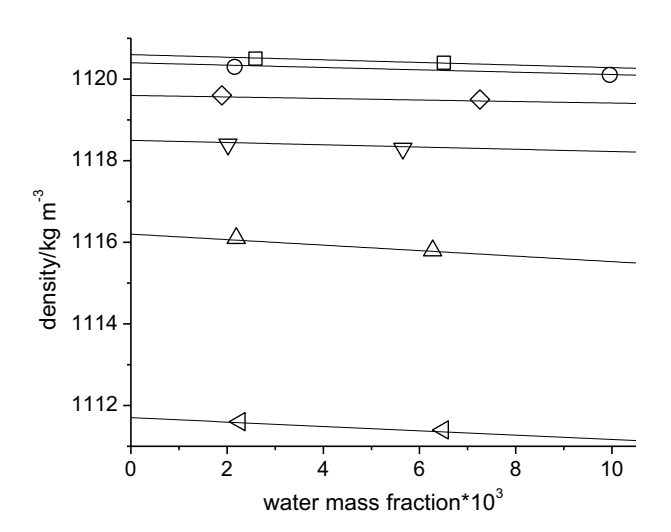




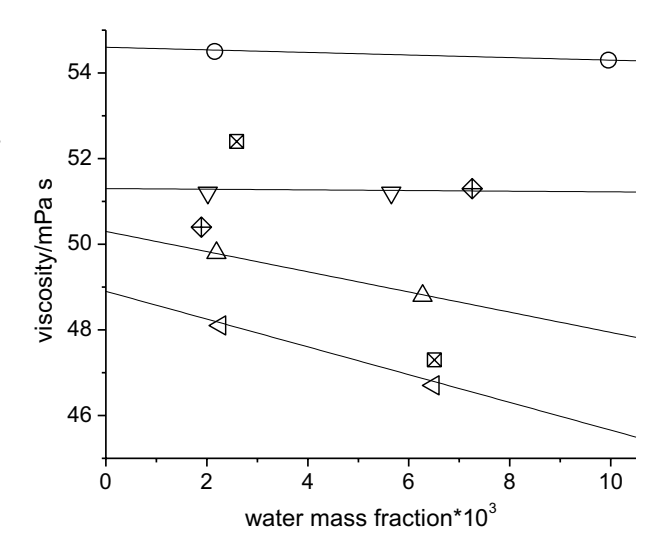
Table 2 Densities in kg⋅m⁻³ of studied solutions

	C					
TEMPO (from MI	P Biochemicals)	in PEG200				
$\overline{T/K \cdot c/mol \cdot L^{-1}}$	0.0106	0.0191	0.0399	0.0761	0.1460	0.2872
298.15	1120.6	1120.4	1119.6	1118.5	1116.2	1111.7
308.15	1112.7	1112.3	1111.7	1110.5	1108.4	1103.8
318.15	1104.8	1104.4	1103.7	1102.6	1100.3	1096.0
328.15	1096.8	1096.6	1095.8	1094.7	1092.4	1087.9
338.15	1088.9	1088.5	1087.8	1086.7	1084.4	1080.1
348.15	1080.9	1080.5	1079.8	1078.7	1076.3	1072.1
358.15	1072.9	1072.5	1071.8	1070.7	1068.4	1064.1
TEMPO (from A	A Blocks) in PEG	200				
$T/K\c/mol\cdot L^{-1}$	0.0076	0.0222	0.0472	0.0927	0.1755	0.3379
298.15	1120.6	1120.2	1119.4	1117.5	1115.1	1110.3
308.15	1112.6	1112.2	1111.4	1109.6	1107.0	1102.4
318.15	1104.7	1104.3	1103.5	1101.6	1099.1	1094.4
328.15	1096.7	1096.2	1095.5	1093.7	1091.1	1086.5
338.15	1088.8	1088.3	1087.6	1085.8	1083.2	1078.5
348.15	1080.8	1080.3	1079.6	1077.8	1075.2	1070.5
358.15	1072.8	1072.4	1071.6	1069.8	1067.2	1062.5
TBIPA in PEG200	0					
$T/K\c/mol\cdot L^{-1}$	0.0090	0.0193		0.0417	0.0789	0.1441
298.15	1121.4	1121.2		1121.5	1121.9	1123.0
308.15	1113.6	1113.3		1113.5	1114.0	1115.1
318.15	1105.5	1105.3		1105.6	1106.0	1107.2
328.15	1097.6	1097.4		1097.7	1098.1	1099.3
338.15	1089.6	1089.4		1089.7	1090.2	1091.4
348.15	1081.8	1081.5		1081.7	1082.2	1083.4
358.15	1073.6	1073.4		1073.7	1074.2	1075.4

the average of the two viscosities at different water mass fraction was chosen as the best estimate for the viscosity of dry PEG200 solution. Thus, the repetition of the viscosity measurements after addition of some water also serves in this case to identify outlying viscosity data. The viscosities of the "dry" PEG200 solutions are listed in Table 3. Although the dependency of density and viscosity on water mass fraction is very small, it appears to be stronger for the PEG200 solutions in this study than for neat PEG200 because the magnitude of the slope values listed in Tables S2–S7 is still somewhat larger compared to what was reported for neat PEG200 [14]. As for the self-diffusion coefficients, the measurement uncertainties are insufficient for reasons as explained in Sect. 2 to allow distinction between the measurement results before and after water addition. Thus, the self-diffusion coefficients of "dry" PEG200 listed in Table 4 were taken as the average of the two sets of measurements of different water mass fractions. The self-diffusion coefficients in Table 4 are shown at the same temperatures for which density and viscosity values were measured. To obtain these values, interpolation from the temperature dependence of the self-diffusion coefficients, (see next subsection), was



Fig. 2 Viscosities of solutions of TEMPO in PEG200 at 298.15 K as a function of water mass fraction of present water at TEMPO concentrations of 0.0106 (squares with cross), 0.0191 (circles), 0.0399 (diamonds with plus), 0.0761 (down triangles), 0.1460 (up triangles), and 0.2872 (left triangle) mol·l⁻¹



necessary. The raw self-diffusion data obtained at actual measurement temperatures are listed in Tables S8–S10.

3.2 Temperature Dependence

A prior study of neat PEG200 found a linear temperature dependence for density while viscosities and self-diffusion coefficients followed the Arrhenius law over the investigated temperature range [14]. Linear temperature dependence of the density is also clearly indicated for all of the PEG200 solutions in this study as shown in Fig. 3. Moreover, the molar volumes are also found to be linearly dependent on temperature. This allows for the calculation of the isobaric thermal expansion coefficients, α , an important material property, from the slope of the linear temperature dependence of the molar volumes, \overline{V} , according to Eq. 2.

$$\alpha = \frac{1}{V} \left(\frac{\partial \overline{V}}{\partial T} \right)_P \tag{2}$$

The values for α are listed in Table S12. It is noteworthy in Fig. 3 that the addition of 5-TBIPA increases the densities compared to neat PEG200, while the addition of TEMPO decreases the densities. The concentration dependence of the physical properties is inspected in more detail in Sect. 3.3.

Figure 4 inspects if the temperature dependence of the viscosity and the self-diffusion coefficients of various PEG200 solutions obtained in this study follow the Arrhenius law, or if they are better described by the Vogel–Fulcher–Tammann (VFT) equation [54]. The Arrhenius and VFT equations are shown in logarithmic form in Eqs. 3 and 4, respectively.

$$\ln(X(T)) = \ln A \pm \frac{E_a}{RT} \tag{3}$$



Table 3 Viscosities in mPa·s of studied PEG200 solutions

TEMPO (from MI	P biochemical) i	n PEG200				
$T/K\c/mol\cdot L^{-1}$	0.0106	0.0191	0.0399	0.0761	0.1460	0.2872
298.15	52.8	54.6	50.8	51.3	50.3	48.9
308.15	33.0	33.8	32.0	32.5	31.6	31.1
318.15	22.1	22.4	21.3	21.9	21.2	20.2
328.15	14.6	15.1	14.5	14.3	14.0	13.6
338.15	10.6	11.0	10.6	10.4	10.2	9.9
348.15	8.0	8.3	8.0	7.9	7.7	7.5
358.15	6.2	6.4	6.2	6.1	6.0	5.9
TEMPO (from AA	A Blocks) in PE	G200				
$T/K\c/mol\cdot L^{-1}$	0.0076	0.0222	0.0472	0.0927	0.1755	0.3379
298.15	52.8	52.6	52.0	49.9	49.1	47.5
308.15	33.3	33.7	32.6	31.6	31.5	30.3
318.15	22.3	22.5	21.7	21.0	21.3	19.6
328.15	14.7	14.8	14.5	14.2	13.9	13.5
338.15	10.7	10.7	10.6	10.4	10.2	9.9
348.15	8.0	8.1	8.0	7.8	7.7	7.4
358.15	6.2	6.4	6.2	6.1	6.0	5.8
5-TBIPA in PEG2	00					
$T/K\c/mol\cdot L^{-1}$	0.0090	0.0193	3	0.0417	0.0789	0.1441
298.15	53.9	54.6		55.1	56.6	63.1
308.15	34.2	33.9		35.0	34.5	38.7
318.15	23.0	22.6		23.1	22.9	24.9
328.15	15.0	15.4		15.3	15.6	16.6
338.15	10.8	11.1		11.1	11.2	12.0
348.15	8.1	8.3		8.3	8.5	9.0
358.15	6.3	6.4		6.4	6.6	6.9

$$\ln(X(T)) = \ln y_0 \pm \frac{B}{(T - T_0)} \tag{4}$$

In Eqs. 3 and 4, X(T) represents the temperature-dependent property. Because viscosity increases with 1/T but self-diffusion decreases, the sign before the second term of the right-hand equation is positive for viscosity and negative for the self-diffusion coefficients. The fit parameters E_a and A, and y_0 , B and T_0 are material dependent where E_a is the activation energy, A and y_0 are pre-exponential factors, B represents the fragility strength coefficient, and T_0 is referred to as the Vogel divergence temperature. Shown in Fig. 4 are the data for the highest concentrated samples measured. Compared to the temperature dependencies of neat PEG200, which is included in Fig. 4 as solid lines, some slight deviations from linearity over the investigated temperature ranges are indicated for both viscosity and self-diffusion coefficients. Given



Table 4 Self-diffusion coefficients in 10^{-10} m²·s⁻¹ of studied PEG200 solutions

PEG200 from soluti	on of TEMPO (fro	om MP Bio) in PEO	G200			
$\overline{T/K \setminus c/\text{mol} \cdot L^{-1}}$		0.0106	0.0191	[0.0399	
298.15		0.26			0.25	
308.15		0.42	0.40		0.45	
318.15		0.63	0.63		0.69	
328.15		0.92	0.92		0.97	
338.15		1.29	1.30	1.28		
348.15		1.75	1.77		1.62	
358.15		2.33	2.34		1.95	
PEG200 from soluti	on of TEMPO (fro	om AABlocks) in F	PEG200		-	
$\overline{T/K\setminus c/\text{mol}\cdot L^{-1}}$		0.0076	0.0222	2	0.0472	
298.15		0.27	0.16		0.15	
308.15		0.43	0.40		0.33	
318.15		0.65			0.58	
328.15		0.94		0.98		
338.15		1.30		1.25		
348.15		1.73		1.50		
358.15		2.23		1.72		
PEG200 from soluti	on of TBIPA in Pi	EG200				
$T/K \ c/mol \cdot L^{-1}$	0.0090	0.0193	0.0417	0.0789	0.1441	
298.15	0.26	0.26	0.26	0.24	0.22	
308.15	0.42	0.42	0.42	0.40	0.38	
318.15	0.65	0.63	0.63	0.62	0.59	
328.15	0.93	0.91	0.91	0.89	0.84	
338.15	1.28	1.25	1.24	1.22	1.14	
348.15	1.68	1.65	1.63	1.63 1.60		
358.15	2.15	2.13	2.08	2.04	1.85	
5-TBIPA from soluti	ion of 5-TBIPA in	PEG200				
$T/K \ c/mol \cdot L^{-1}$	0.0090	0.0193	0.0417	0.0789	0.1441	
298.15	0.11	0.12	0.12	0.11	0.11	
308.15	0.20	0.20	0.20	0.20	0.19	
318.15	0.31	0.32	0.31	0.31	0.30	
328.15	0.45	0.46	0.45	0.46	0.44	
338.15	0.60	0.62	0.64	0.65	0.62	
348.15	0.76	0.81	0.86	0.87	0.83	
358.15	0.94	1.02	1.14	1.12	1.07	

the observation that deviations from Arrhenius behavior are only small, Tables 5 and 6 list the fit parameters for both Eqs. 3 and 4 for viscosity and self-diffusion coefficients, respectively. The obtained activation energies are generally not significantly different from one another, regardless of the type of PEG200 solution, solute concentration and



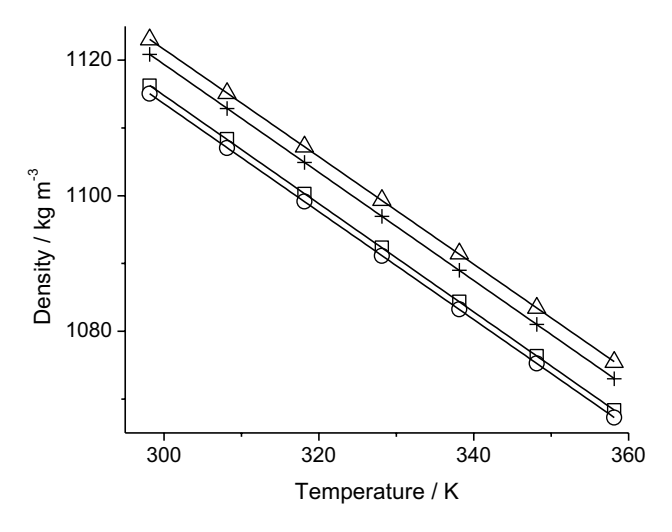
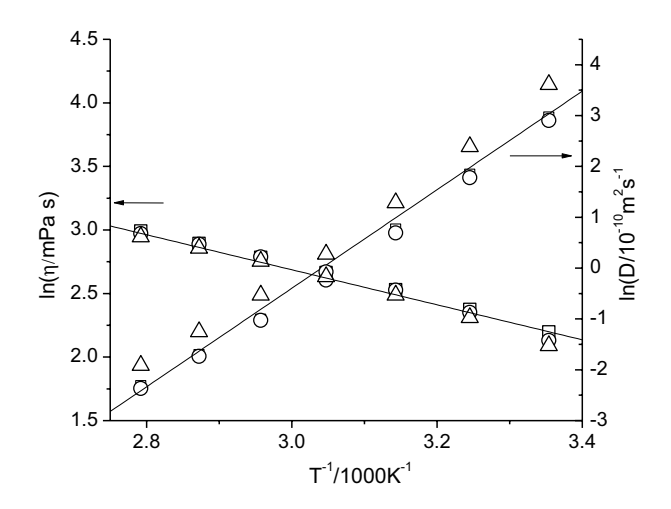


Fig. 3 Temperature dependence of density for solutions of 0146 molar from MP Biochemical in PEG200 (square), 0.176 molar TEMPO from AA Blocks in PEG200 (circle), 0.144 molar 5-TBIPA in PEG200 (triangle), and for comparison PEG200 by itself (plus symbols, data taken from Hoffmann et al. [14]). The lines are least linear square fits

Fig. 4 Temperature dependences of viscosity, η , and PEG200 self-diffusion coefficient, D, for the systems of TEMPO from Biochemicals (squares) and AA Blocks (circles) in PEG200, and 5-TBIPA in PEG200 (triangle). The lines are least linear square fits for neat PEG200 taken from Hoffmann et al. [14]



if they concern viscosities or self-diffusion coefficients. The majority of the values in Tables 5 and 6 are between 31–32 kJ·mol⁻¹ except for the self-diffusion coefficients of 5-TBIPA that monotonically increase to 33.7 kJ·mol⁻¹ at 0.144 mol·l⁻¹. These activation energies are similar to those reported for neat PEG200 [14]. The same activation energies for viscosity and self-diffusion were also observed for the neat oligomers [13], which indicates that the activation barrier for translation motion is the same as for momentum transfer. This appears to hold also for the PEG200 solutions except perhaps for the 5-TBIPA component. It is interesting to observe in Fig. 4 that the effect on the viscosity by addition of TEMPO is relatively minor compared to adding 5-TBIPA,



$c/\text{mol}\cdot L^{-1}$	ln(A/mPa·s)	$E_{\rm a}/{\rm kJ\cdot mol^{-1}}$	$\sigma_{ m Arrh}$	y₀/mPa·s	B/K	T ₀ /K	$\sigma_{ m VFT}$
TEMPO (fro	om MP Bio) in PE	EG200					
0.0106	-8.92	31.8	0.02	0.0477	948.5	163.0	0.009
0.0191	-8.82	31.6	0.02	0.0654	863.4	169.9	0.006
0.0399	-8.69	31.2	0.02	0.0526	931.9	162.7	0.004
0.0761	-8.89	31.7	0.02	0.0379	1022.9	156.6	0.012
0.1460	-8.87	31.6	0.02	0.0501	927.4	164.1	0.010
0.2872	-8.88	31.5	0.02	0.0651	837.4	171.9	0.009
TEMPO (fro	om AA Blocks) in	PEG200					
0.0076	-8.93	31.9	0.02	0.0391	1014.9	157.5	0.010
0.0222	-8.78	31.5	0.02	0.0500	949.3	162.0	0.013
0.0472	-8.87	31.6	0.02	0.0502	934.8	163.7	0.007
0.0927	-8.76	31.3	0.02	0.0467	960.9	160.5	0.006
0.1755	-8.83	31.5	0.02	0.0306	1095.9	149.9	0.012
0.3379	-8.81	31.3	0.02	0.0525	905.9	165.3	0.006
5-TBIPA in	PEG200						
0.0090	-8.99	32.1	0.02	0.0302	1103.3	151.0	0.012
0.0193	-9.02	32.2	0.02	0.0426	1001.0	158.3	0.006
0.0417	-8.96	32.1	0.02	0.0347	1063.2	154.1	0.009
0.0789	-10.44	36.4	0.02	0.0711	840.2	172.4	0.003
0.1441	-9.12	32.7	0.02	0.0718	837.4	174.7	0.006

Table 5 Arrhenius and VFT fit parameters for temperature dependence of viscosity

where nevertheless the points run nearly parallel to the line representing neat PEG200. The PEG200 self-diffusion coefficients are even less sensitive to the addition of solute. As for the self-diffusion coefficients of 5-TBIPA, these are noticeably smaller than the corresponding PEG200 self-diffusion coefficients. A closer inspection on the solute concentration dependence of viscosity and self-diffusion is provided in the next subsection.

3.3 Solute Concentration Dependence

As can be observed in Table 2, the addition of TEMPO to PEG200 results in a lowering of the solution density, while the addition of 5-TBIPA does the opposite. Since the solution molar volume is inversely proportional to the solution density, one would expect that the molar volume of the solutions should then increase with addition of TEMPO and decrease with the addition of 5-TBIPA. However, the average molar weight of the PEG200 solution also changes with addition of solute. Because TEMPO has with 157.26 g·mol⁻¹ a smaller molar weight than PEG200, adding it to PEG200 decreases the average molar weight of the solution. The opposite is true for 5-TBIPA addition, which has with 222.24 g·mol⁻¹ a larger molar weight than PEG200. The decreasing average molar weight outweighs the density decrease with TEMPO addition, and the molar volume overall decreases with TEMPO concentration, as can be seen in Fig. 5. For 5-TBIPA, the density increase and the average molar weight increase upon its addition to PEG200 essentially cancel each other, and thus, the molar volume is nearly flat in Fig. 5.



0.0789

0.1441

11.3

11.2

31.3

31.3

 1.4×10^{-4}

 5.6×10^{-4}

c/mol·L ⁻¹	$\frac{\ln(A/10^{-10})}{\text{m}^2 \cdot \text{s}^{-1}}$	$E_{\rm a}/{\rm kJ\cdot mol^{-1}}$	$\sigma_{ m Arrh}$	$y_0/10^{-10} \text{ m}^2 \cdot \text{s}^{-1}$	B/K	T_0/K	$\sigma_{ m VFT}$
PEG as solv	ent of TEMPC	(from MP Bio)	,				
0.0106	11.6	32.1	0.021	267.7	917.9	166.3	1.6×10^{-4}
0.0191	11.9	32.8	0.024	222.4	841.7	174.6	1.2×10^{-4}
0.0399	10.6	29.3	0.017	213.9	928.9	157.9	9.0×10^{-4}
PEG as solv	ent of TEMPC	(from AA Block	cs)				
0.0076	11.4	31.4	0.029	93.5	622.6	192.5	8.2×10^{-5}
0.0222	11.8	32.6	0.067	13.5	214.1	246.8	1.9×10^{-3}
0.0472	11.1	30.8	0.042	28.8	366.6	221.6	4.8×10^{-4}
5-TBIPA as	solute in PEG	200					
0.0090	10.5	31.1	0.050	9.6	292.0	232.6	2.3×10^{-4}
0.0193	10.7	31.6	0.036	25.8	484.2	208.2	1.9×10^{-4}
0.0417	11.2	32.8	0.019	215.3	1057.6	156.5	2.6×10^{-4}
0.0789	11.4	33.5	0.032	53.5	626.2	196.2	4.6×10^{-5}
0.1441	11.4	33.7	0.031	59.2	662.6	192.9	8.3×10^{-6}
PEG200 as	solvent of 5-TE	BIPA					
0.0090	11.4	31.4	0.028	100.4	646.9	189.9	9.3×10^{-5}
0.0193	11.3	31.1	0.021	198.1	855.6	169.4	1.4×10^{-5}
0.0417	11.1	30.7	0.024	122.1	720.8	181.1	1.7×10^{-5}

Table 6 Arrhenius and VFT fit parameters for temperature dependence of self-diffusion

It is useful to inspect the apparent molar volume of the solute component, $\overline{V}_{2,\phi}$, as defined in Eq. 5 [55], to get a better sense for the molar volume contributions from the solute. In Eq. 5, M_2 is the molar mass, ρ and ρ_0 are densities of solution and solvent, respectively, and m_2 is the solute molality in mol·kg⁻¹.

80.3

34.7

0.030

0.039

$$\overline{V}_{2,\phi} = \frac{M_2}{\rho} - \frac{1000(\rho - \rho_0)}{m_2 \rho \rho_0} \tag{5}$$

600.6

417.7

194.6

215.8

The number values for the apparent molar volumes are listed in Table S14, and Fig. 6 shows the concentration dependence of the apparent molar volume at 298.15 K. It should be noted that the uncertainty of the apparent molar volume values increases with decreasing solute concentration because the density difference as well the molality approaches zero for infinitely dilute solutions. Therefore, the data points for the lowest concentrations in Fig. 6, especially the value of 142 cm³·mol⁻¹ for 5-TBIPA, should probably be ignored. At higher concentrations, the apparent molar values plateau to a steady value. The apparent molar volume values should be distinctly larger for 5-TBIPA because of its larger molar weight. However, the second term in Eq. 5 contributes significantly as well to the apparent molar volume. This second term is additive in the case of TEMPO because its addition decreases the system density, while the second term is subtracted from the first term in Eq. 5 in the case of 5-TBIPA because its addition increases the system density compared to neat PEG200. Thus, the apparent molar volumes in Fig. 6 are only ~20 cm³·mol⁻¹ larger for 5-TBIPA compared to TEMPO and about the same value as the solution molar volumes. Thus, Fig. 6 suggests that 5-TBIPA as a solute contributes about equally to the



Fig. 5 Solution molar volume at 298.15 K as a function of molarity of TEMPO (from BP Bio as squares and AA Blocks as circles) and 5-TBIPA (triangle) in PEG200. The molar volume of neat PEG200 (zero solute molarity) is included (solid diamond). The lines are guides to the eye

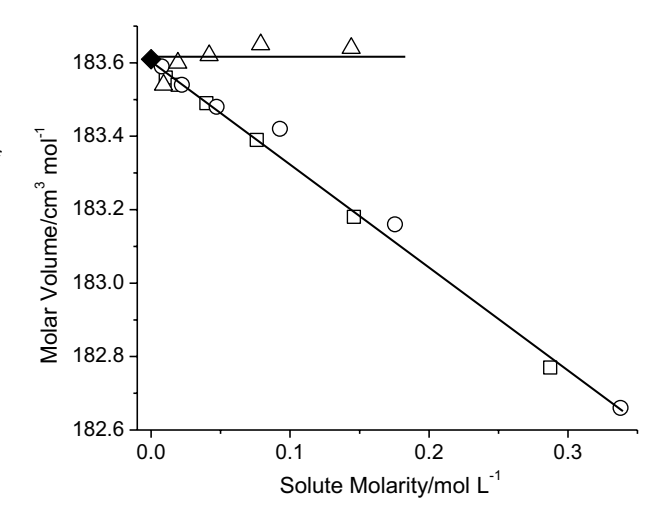
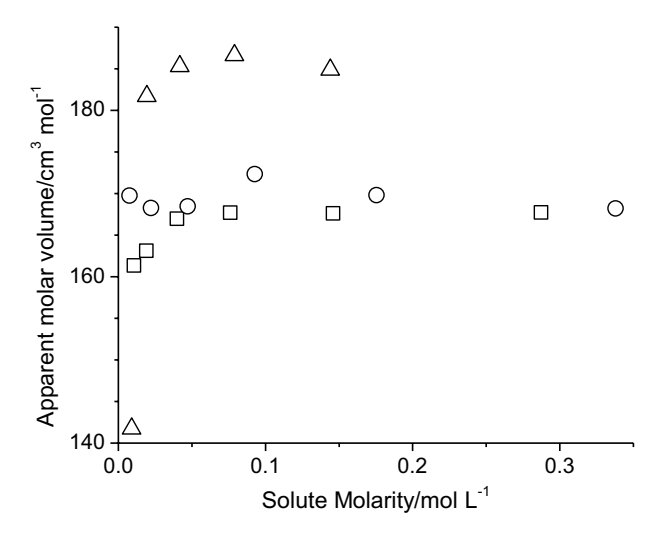


Fig. 6 Apparent molar volume at 298.15 K as a function of molarity of TEMPO (from BP Bio as squares and AA Blocks as circles) and 5-TBIPA (triangle) in PEG200



molar volume of the solution as the PEG200 solvent, which is confirmed in Fig. 5 with the unchanging molar solution volume when 5-TBIPA is added. The apparent molar volume of TEMPO is smaller than the molar volume of neat PEG, which is in keeping with the observation in Fig. 5 that the solution molar volume decreases upon addition of TEMPO. Finally, we point out that the solute partial molar volume, \overline{V}_2 , is related to the solute apparent volume as shown in Eq. 6 [55].

$$\overline{V}_2 = \overline{V}_{2,\phi} + n_2 \frac{\partial \overline{V}_{2,\phi}}{\partial n_2} \tag{6}$$

Given that the derivative term in Eq. 6 is approximately zero for the observed flat concentration dependence of the solute apparent molar volumes in Fig. 6, the partial and apparent molar solute volumes are approximately equal for these concentration regions in Fig. 6.



Fig. 7 Viscosities at 298.15 K as a function of molarity of TEMPO (from BP Bio as squares and AA Blocks as circles) and 5-TBIPA (triangle) in PEG200. The viscosity of neat PEG200 (zero solute molarity) reported by Hoffmann et al. [14] is included (solid diamond). The solid lines are guides to the eye

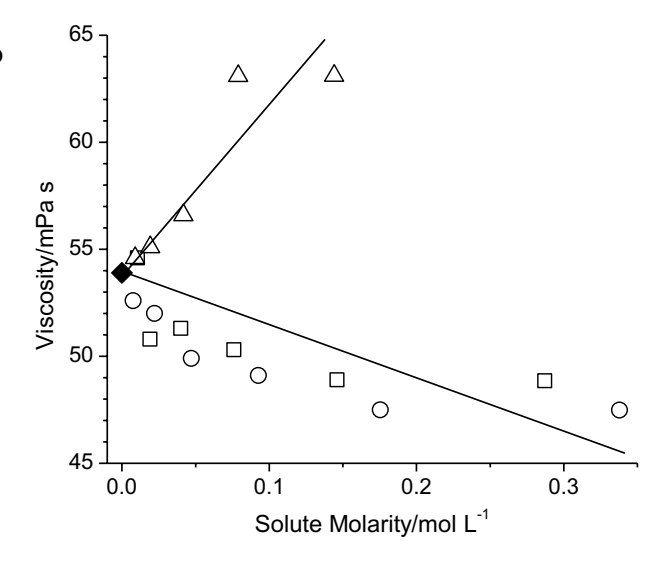
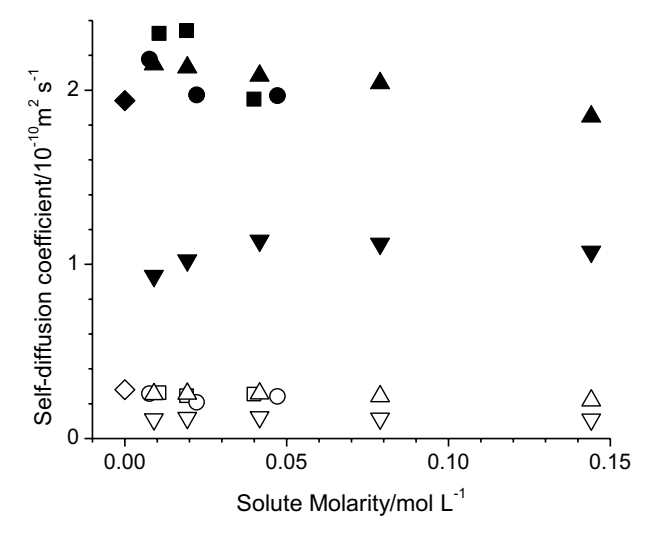


Fig. 8 Self-diffusion coefficients of PEG200 at 298.15 K (open symbols) and at 358.15 K (solid symbols) as a function of molarity of TEMPO (from BP Bio as squares and AA Blocks as circles) and 5-TBIPA (up triangles) in PEG200. Self-diffusion coefficients of 5-TBIPA are shown as well (down triangles). The shown self-diffusion coefficients of neat PEG200 (solid diamonds) were taken from Hoffmann et al. [14]



The already mentioned increasing uncertainty of $\overline{V}_{2,\phi}$ as solute concentration approaches zero does not allow a reliable evaluation of \overline{V}_2 for very low solute concentrations.

Similar to density, the system viscosity also displays an opposite response to the addition of solute. As can be seen in Fig. 7, addition of TEMPO lowers the solution viscosity, while addition of 5-TBIPA increases it. The concentration dependence of the PEG200 self-diffusion coefficient is shown in Fig. 8 for the lowest temperature of 298.15 K as well as the highest temperature of 358.15 K. Figure 8 shows that the PEG self-diffusion coefficient is essentially flat upon addition of TEMPO as well as upon the addition of 5-TBIPA. The self-diffusion coefficients of 5-TBIPA are included in Fig. 8 (TEMPO is not observable as explained in the experimental section), which shows that the 5-TBIPA solute self-diffuses about half as fast as the PEG200 solvent medium. These qualitative trends for the



concentration dependence of the self-diffusion coefficients are consistently observable at each measured temperature.

According to the Stokes-Einstein equation

$$D = \frac{k_B T}{\xi \pi \eta r} \tag{7}$$

the self-diffusion coefficient, D, is inversely proportional to the viscosity, η , of the medium. The fact that the self-diffusion coefficients of the PEG200 solvent (as well as the 5-TBIPA solute) are essentially unchanged upon addition while the solution viscosity increases or decreases depending on solute seems to contradict the Stokes–Einstein Equation. It is principally conceivable that 5-TBIPA might form dimers through the carboxylic acid functional groups. This would lead to an increase in its hydrodynamic radius, r, typically taken to be the van der Waals radius [56], in Eq. 7 where k_B is the Boltzmann constant, T the temperature, and ξ is a constant that ranges between a value of 4 for the so-called slip boundary condition where there are no interactions between the self-diffusing particle, and a value of 6 for the stick boundary conditions where these interactions are strong [57]. Besides possible interactions between the self-diffusing particles, the constant ξ is also influenced by the ratio of solvent and solute radius, r_{soly}/r [58], as can be seen in Eq. 8 that was derived by Chen and Chen [59] from the microfriction theory by Gierer and Wirtz [60].

$$\xi = \frac{6}{1 + 0.695 \left(\frac{r_{solv}}{r}\right)^{2.234}} \tag{8}$$

Equations 7 and 8 were iteratively solved to obtain the values for ξ and r, respectively, listed in Tables S15 and S16 in the supplementary materials. A value of 3.548×10^{-10} m was used as r_{soly} for the polydisperse PEG200 solvent, which was obtained first by evaluating the van der Waals radii of each ethylene glycol oligomer using the method by Bondi [61] as further detailed by Edwards [62] and then taking the mole fraction weighted average of these oligomer radii according to the prior reported composition analysis of PEG200 [14], which for convenience is tabulated in Table S1. The use of a mol fraction weighted average value for r_{solv} is justifiable in so far that the time of the NMR measurement (on the order of a second) is much longer than the motional dynamics of the system, which thus averages out the PEG solvent component the solute molecule experiences during the NMR measurement. We note that the value for r_{soly} of 3.548×10^{-10} m is close to the values of 3.440×10^{-10} and 3.872×10^{-10} m obtained, respectively, from mole fraction weighted averages of reported radii of gyration and end-to-end distances (divided by 2) of the individual ethylene glycol oligomers that were reported in a recent MD simulation study of PEG200 [63]. However, when evaluating r_{solv} from viscosity and self-diffusion data reported for neat PEG200 [14] using Eq. 7, they increase from 2.17×10^{-10} m at 298.15 K to 3.2×10^{-10} m at 358.15 K using a value of 4 for ξ and would be even smaller by 1/3 if using a value of 6 for ξ . These values are considerably smaller than 3.548×10^{-10} m, which suggests that the smaller ethylene glycol oligomers contribute more to the overall mass transport in neat PEG200 than the larger ones. Nevertheless, the value of 3.548×10^{-10} m was used for r_{solv} to be consistent in using the Bondi method for evaluating both the solvent and solute hydrodynamic radii.

The values for ξ in Table S15 range between 4.3 and 4.8, and the values for r in Table S16 range between 4.6×10^{-10} and 5.5×10^{-10} m. The values for both ξ and r generally increase with increasing temperature but decrease with 5-TBIPA concentration. The



values of r in Table S16 exceed the van der Waals radius of 3.65×10^{-10} m obtained from the Bondi method by up to 1.5×10^{-10} m, which might be an indication that some of the dissolved 5-TBIPA are present as dimers. However, higher temperatures and lower concentrations should shift the equilibrium away from these species, if present, toward the single 5-TBIPA species. The contrary is observed for the entries of r in Table S16. In fact, the decrease in r with increasing 5-TBIPA reflects the concurrent viscosity increase as observed in Fig. 7. We also note that using a smaller value for r_{soly} would lead to smaller values of r in Table S16. Specifically, if the r_{soly} value were indeed overestimated by for example 1×10^{-10} m, the values of ξ in Table S15 would increase by about 0.5 and the values for r in Table S16 would decrease by about 0.5×10^{-10} m. Thus, it appears more reasonable that the potential presence of 5-TBIPA dimers can be neglected and reasons other than the presence of dimers or aggregate equilibrium species need to be considered for explaining why the self-diffusion coefficients of the PEG200 solvent as well as the 5-TBIPA solute are not inversely proportional to the solution viscosity. Hereto, we note that a decoupling of translational motion from the medium viscosity has been observed for glass forming liquids [64, 65], and PEG200 is a glass forming liquid [66]. Normally, such behavior would not be observable at the temperature ranges investigated in this study, but much lower temperatures that approach the glass transition temperature. However, deviations from the Stokes-Einstein equation have been observed for a number of other solutions including aqueous solutions, as pointed out in other reports [67, 68], as well as for small solutes in viscous solutions [69]. Hence, the observed behavior of the PEG solutions studied here may not all be unusual but instead be just another example of a binary system not following the Stokes–Einstein equation. A likely reason for the observed concentration independence of the self-diffusion coefficients is based on the consideration of solute-solvent interactions that is presented in the next subsection.

3.4 Molecular-Level Interpretation

When a solute is added to a solvent, the solvent will need to reorganize around the introduced solute accommodating the needed space and responding to the newly present intermolecular interactions with the solute, which may be attractive or repulsive in nature. Theories such as the Prigorine-Flory-Patterson (PFP) theory account for these contributions to the solution density but may not include specific interactions such as hydrogen bonding [70]. Given that PEG possesses terminal hydroxy functional groups, hydrogen bonding interactions are expected to be a major if not the dominating factor in explaining the observed changes in the physical properties. In this respect, a recent molecular dynamics study of PEG200 has shown that PEG200 not only engages in intermolecular hydrogen bonding but also significantly in intramolecular hydrogen bonding both of which have profound influence on viscosity and self-diffusion [63]. The chemical structure of TEMPO includes with the nitroxyl moiety only one functional group that can accept a proton in hydrogen bonding interactions. The 5-TBIPA chemical structure includes two carboxyl groups that can accept as well as donate a proton in hydrogen bonding interactions. Especially at the lowest investigated solute concentrations, the solutes are dominantly interacting with the PEG solvent, as already discussed in Sect. 3.3 in the context of the observed solute radii. Hence, we will focus the discussion here on solute-solvent intermolecular interactions. In this regard, it is important to point out that only 5-TBIPA can engage in hydrogen bonding with the ether moieties of PEG200, while TEMPO may only accept a proton from the PEG200 hydroxy terminal group. For these molecular structural



reasons, 5-TBIPA should more likely engage in hydrogen bonding than TEMPO. Moreover, 5-TBIPA could engage in bridging hydrogen bonding where it is hydrogen bonded to more than one ethyleneglycol oligomer component of PEG200. Combined, these considerations to the intermolecular solute–solvent interactions would explain the observed increase in density and viscosity upon addition of 5-TBIPA to PEG200, while the weaker hydrogen bonding interactions of TEMPO with PEG200 may overall weaken the intermolecular interactions in PEG200 and thus result in lower densities and viscosities.

This leaves then the question why the self-diffusion coefficients in Fig. 8 display solute concentration dependences that are essentially flat. The measured self-diffusion coefficients represent the ensemble and time averaged self-diffusion processes of the PEG200 solvent and the 5-TBIPA solute. It is interesting that the self-diffusion coefficients of 5-TBIPA are about a factor 2 slower than that of the PEG200 solvent consistently at all experimental conditions even though the average van der Waals radius of PEG200 is with 3.55×10^{-10} m about the same as that for 5-TBIPA (3.6×10^{-10} m). Indeed, the calculated (Eqs. 7 and 8) 5-TBIPA radii in Table S16 are significantly larger than 3.6×10^{-10} m, as pointed out in Sect. 3.3. It appears then that on average each 5-TBIPA molecule hydrogen bonds with one ethyleneglycol oligomer in PEG200. Even at 0.15 molar concentration, the 5-TBIPA mole fraction is with 0.0265 rather small. Thus, the PEG200 self-diffusion coefficient, D_{solv} remains essentially unaffected as it is the mole fraction weighted contribution of PEG200 oligomers by themselves, D_{PEG200} , and those that are hydrogen bonded with 5-TBIPA, $D_{\text{PEG200},hb}$, as shown in Eq. 9.

$$D_{solv} = x_{PEG200}D_{PEG200} + x_{PEG200,hb}D_{PEG200,hb}$$
(9)

Compared to the first term in Eq. 9, the second term is negligibly small mainly because of the small value of $x_{\text{PEG200},hb}$ in addition to the consideration that $D_{\text{PEG200},hb} = D_{5\text{-TBIPA}} \approx \frac{1}{2} D_{\text{PEG200}}$. $D_{5\text{-TBIPA}}$ also shows solute concentration independence because the situation of each additional added 5-TBIPA molecule in terms of its intermolecular interaction with the PEG200 solvent is the same since solute–solute interactions appear to be not significant for the investigated concentration range.

4 Conclusions

New experimental densities, viscosities, and self-diffusion coefficients were obtained for solutions of PEG200 with TEMPO and 5-TBIPA as solutes to contribute to a better understanding of PEG200 as a benign chemical medium. These properties are hardly affected by the presence of water, the main impurity of PEGs given their propensity to absorb moisture from air. Density decreases linearly with temperature, while self-diffusion coefficients and viscosity display slight deviations from the Arrhenius equation over the investigated temperature range. The activation energy barriers for translational motion and momentum transfer appear to be identical and are hardly affected by the addition of the solute. Addition of TEMPO decreases the solution density and viscosity while the opposite is observed when 5-TBIPA is added. An explanation has been provided for this opposite behavior in terms of the solute–solvent interactions based on the molecular structural differences between TEMPO and 5-TBIPA. Strong intermolecular interactions, likely hydrogen bonding interactions, between 5-TBIPA and PEG200 are indicated based on the observation that 5-TBIPA self-diffuses at about half the rate as the PEG200 solvent despite their similar hydrodynamic radii. However, only a small mole fraction of the PEG200 oligomers is



affected by these intermolecular interactions rendering their observed self-diffusion coefficients essentially independent to the solute concentration. This concentration independence of the self-diffusion coefficient, while concurrent increase in viscosity with 5-TBIPA concentration, is inconsistent with the Stokes–Einstein equation. Nevertheless, the use of the Stokes–Einstein results in solute radii, and concentration and temperature dependences thereof, that support the absence of significant solute–solute interactions but instead support the presence of strong solute–solvent interactions in the case of 5-TBIPA in PEG200. Overall, it appears that the addition of TEMPO weakens the intermolecular interactions present in the PEG200 solutions while the addition of 5-TBIPA strengthens them. Finally, it should be pointed out that this study illustrates how much is generally unknown about the intermolecular interactions present in PEG solutions. Many more experimental and theoretical studies are needed to elucidate the structure and dynamics of PEG solutions before challenging research topics such as PEG solvent effects on reaction kinetics can be tackled.

Supplementary Information The online version contains supplementary material available at https://doi.org/10.1007/s10953-023-01265-4.

Author Contributions Conceptualization, methodology, and supervision were performed by MH; formal analysis and investigation by NR, NP, MA, MH; writing—original draft preparation—by MH; writing—review and editing—by MH, NR, MA, NP, TG, and GB; funding acquisition by GB, TG, MH; resources by MH, GB.

Funding This report is based upon work supported by the National Science Foundation under Grant No. [1953428] and the Deutsche Forschungsgemeinschaft (DFG) under grant Bu 911/24-2. The latter included a Mercator fellowship for MMH to support research stays at the Technical University Darmstadt.

Data Availability All data generated or analyzed during this study are included in this published article [and its supplementary information files].

Declarations

Conflict of interest The authors declare no competing financial interest.

References

- Kardooni, R., Kiasat, A.R.: Polyethylene glycol as a green and biocompatible reaction media for the catalyst free synthesis of organic compounds. Curr. Org. Chem. 24(12), 1275–1314 (2020). https://doi. org/10.2174/1385272824999200605161840
- Campos, J.F., Berteina-Raboin, S.: Greener synthesis of nitrogen-containing heterocycles in water, PEG, and bio-based solvents. Catalysts 10(4), 429 (2020). https://doi.org/10.3390/catal10040429
- Soni, J., Sahiba, N., Sethiya, A., Agarwal, S.: Polyethylene glycol: A promising approach for sustainable organic synthesis. J. Mol. Liq. 315, 113766 (2020). https://doi.org/10.1016/j.molliq.2020.113766
- Polyethylene glycol market size, share & trends analysis report by application (medical, personal care, industrial), by region (North America, Europe, Asia Pacific, Row), and segment rorecasts, 2015–2020. https://www.grandviewresearch.com/industry-analysis/polyethylene-glycol-peg-market Accessed 07/08/2021.
- Gullapalli, R.P., Mazzitelli, C.L.: Polyethylene glycols in oral and parenteral formulations
 –a critical review. Int. J. Pharm. 496(2), 219–239 (2015). https://doi.org/10.1016/j.ijpharm.2015.11.015
- Hutanu, D.: Recent applications of polyethylene glycols (PEGs) and PEG derivatives. Mod. Chem. Appl. 2(2), 6 (2014). https://doi.org/10.4172/2329-6798.1000132
- Kong, X.B., Tang, Q.Y., Chen, X.Y., Tu, Y., Sun, S.Z., Sun, Z.L.: Polyethylene glycol as a promising synthetic material for repair of spinal cord injury. Neural. Regen. Res. 12(6), 1003–1008 (2017). https://doi.org/10.4103/1673-5374.208597



- Calvo-Flores, F.G., Monteagudo-Arrebola, M.J., Dobado, J.A., Isac-Garcia, J.: Green and bio-based solvents. Top. Curr. Chem. 376(3), 18 (2018). https://doi.org/10.1007/s41061-018-0191-6
- McGarvey, P.W., Hoffmann, M.M.: Solubility of some mineral salts in polyethylene glycol and related surfactants. Tens. Surf. Deterg. 55(3), 203–209 (2018)
- Xiong, W.W., Zhang, Q.: Surfactants as promising media for the preparation of crystalline inorganic materials. Angew. Chem. Internat. Edit. 54(40), 11616–11623 (2015). https://doi.org/10.1002/anie. 201502277
- Forsyth, C., Taras, T., Johnson, A., Zagari, J., Collado, C., Hoffmann, M.M., et al.: Microwave assisted surfactant-thermal synthesis of metal-organic framework materials. Appl. Sci. 10(13), 4563 (2020). https://doi.org/10.3390/app10134563
- Hoffmann, M.M.: Polyethylene glycol as a green chemical solvent. Curr. Opin. Colloid Interface Sci. (2022). https://doi.org/10.1016/j.cocis.2021.101537
- Hoffmann, M.M., Horowitz, R.H., Gutmann, T., Buntkowsky, G.: Densities, viscosities, and self-diffusion coefficients of ethylene glycol oligomers. J. Chem. Eng. Data. 66(6), 2480–2500 (2021). https://doi.org/10.1021/acs.jced.1c00101
- Hoffmann, M.M., Kealy, J.D., Gutmann, T., Buntkowsky, G.: Densities, viscosities, and self-diffusion coefficients of several polyethylene glycols. J. Chem. Eng. Data. 67(1), 88–103 (2021). https://doi.org/ 10.1021/acs.jced.1c00759
- Beejapur, H.A., Zhang, Q., Hu, K., Zhu, L., Wang, J., Ye, Z.: TEMPO in chemical transformations: From homogeneous to heterogeneous. ACS Catal. 9(4), 2777–2830 (2019). https://doi.org/10.1021/acscatal.8b05001
- Prakash, N., Rajeev, R., John, A., Vijayan, A., George, L., Varghese, A.: 2,2,6,6-tetramethylpiperidinyloxyl (TEMPO) radical mediated electro-oxidation reactions: A review. ChemistrySelect 6(30), 7691

 7710 (2021). https://doi.org/10.1002/slct.202102346
- Nakagawa, K.: EPR investigations of spin-probe dynamics in aqueous dispersions of a nonionic amphiphilic compound. J. Am. Oil Chem. Soc. 86(1), 1 (2008). https://doi.org/10.1007/s11746-008-1317-8
- Jahnke, W.: Spin labels as a tool to identify and characterize protein-ligand interactions by NMR spectroscopy. ChemBioChem 3(2–3), 167–173 (2002). https://doi.org/10.1002/1439-7633(20020301)3: 2/3%3c167::Aid-cbic167%3e3.0.Co;2-s
- Thankamony, A.S.L., Wittmann, J.J., Kaushik, M., Corzilius, B.: Dynamic nuclear polarization for sensitivity enhancement in modern solid-state NMR. Prog. Nucl. Magn. Reson. Spectrosc. (2017). https://doi.org/10.1016/j.pnmrs.2017.06.002
- Bothe, S., Nowag, J., Klimavičius, V., Hoffmann, M., Troitskaya, T.I., Amosov, E.V., et al.: Novel biradicals for direct excitation highfield dynamic nuclear polarization. J. Phys. Chem. C. 122(21), 11422–11432 (2018). https://doi.org/10.1021/acs.jpcc.8b02570
- Casano G, Karoui H, Ouari O. Polarizing agents: Evolution and outlook in free radical development for DNP. eMagRes. 2018, 195–208.
- Kubicki, D.J., Casano, G., Schwarzwälder, M., Abel, S., Sauvée, C., Ganesan, K., et al.: Rational design of dinitroxide biradicals for efficient cross-effect dynamic nuclear polarization. Chem. Sci. 7(1), 550–558 (2016). https://doi.org/10.1039/C5SC02921J
- Sauvée, C., Casano, G., Abel, S., Rockenbauer, A., Akhmetzyanov, D., Karoui, H., et al.: Tailoring of polarizing agents in the bTurea series for cross-effect dynamic nuclear polarization in aqueous media. Chem. Eur. J. 22(16), 5598–5606 (2016). https://doi.org/10.1002/chem.201504693
- Lund, A., Casano, G., Menzildjian, G., Kaushik, M., Stevanato, G., Yulikov, M., et al.: TinyPols: A family of water-soluble binitroxides tailored for dynamic nuclear polarization enhanced NMR spectroscopy at 18.8 and 21.1 T. Chem. Sci. 11(10), 2810–8 (2020). https://doi.org/10.1039/C9SC05384K
- Mentink-Vigier, F., Marin-Montesinos, I., Jagtap, A.P., Halbritter, T., van Tol, J., Hediger, S., et al.: Computationally assisted design of polarizing agents for dynamic nuclear polarization enhanced NMR: The AsymPol family. J. Am. Chem. Soc. 140(35), 11013–11019 (2018). https://doi.org/10.1021/jacs.8b04911
- Francesconi, R., Ottani, S.: Correlation of density and refraction index for liquid binary mixtures containing polyglycols: Use of the group contributions in the Lorentz–Lorenz, Gladstonez–Dale and Vogel equations to evaluate the density of mixtures. J. Mol. Liq. 133(1–3), 125–33 (2007). https://doi. org/10.1016/j.molliq.2006.07.001
- Comelli, F., Ottani, S.: Excess enthalpies, densities, viscosities, and refractive indices of binary mixtures involving some poly(glycols) + diethyl carbonate at 308.15 K. J. Chem. Eng. Data. 49(4), 970–5 (2004). https://doi.org/10.1021/je0342740
- Adam, O.E.-A.A., Hassan, A.A.: Volumetric properties of binary mixtures of o-cresol + poly(ethylene glycols) in the temperature range 288.15–308.15 K and atmospheric pressure. Phys. Chem. Liq. 56(1), 55–68 (2018). https://doi.org/10.1080/00319104.2017.1292424



- Nain, A.K., Ansari, S., Ali, A.: Densities, refractive indices, ultrasonic speeds and excess properties of acetonitrile + poly(ethylene glycol) binary mixtures at temperatures from 298.15 to 313.15 K. J. Solution Chem. 43(6), 1032–54 (2014). https://doi.org/10.1007/s10953-014-0189-9
- Živković, N.V., Šerbanović, S.S., Kijevčanin, M.L., Živković, E.M.: Volumetric and viscometric behavior of binary systems 2-butanol + PEG 200, + PEG 400, + tetraethylene glycol dimethyl ether, and + N-methyl-2-pyrrolidone. J. Chem. Eng. Data. 58(12), 3332–3341 (2013). https://doi. org/10.1021/je400486p
- Živković, N., Šerbanović, S., Kijevčanin, M., Živković, E.: Volumetric properties, viscosities, and refractive indices of the binary systems 1-butanol + PEG 200, + PEG 400, and + TEGDME. Int. J. Thermophys. 34(6), 1002–1020 (2013). https://doi.org/10.1007/s10765-013-1469-0
- Vuksanović, J.M., Radović, I.R., Šerbanović, S.P., Kijevčanin, M.L.: Experimental investigation of interactions and thermodynamic properties of poly(ethylene glycol) 200/400 + dimethyl adipate/dimethyl phthalate binary mixtures. J. Chem. Eng. Data. 60(6), 1910–1925 (2015). https://doi.org/10.1021/acs.jced.5b00156
- Ali, A., Ansari, S., Nain, A.K.: Densities, refractive indices and excess properties of binary mixtures of dimethylsulphoxide with some poly(ethylene glycol)s at different temperatures. J. Mol. Liq. 178, 178–184 (2013). https://doi.org/10.1016/j.molliq.2012.12.002
- 34. Comelli, F., Ottani, S., Francesconi, R., Castellari, C.: Densities, viscosities, refractive indices, and excess molar enthalpies of binary mixtures containing poly(ethylene glycol) 200 and 400 + dimethoxymethane and + 1,2-dimethoxyethane at 298.15 K. J. Chem. Eng. Data. 47(5), 1226–31 (2002). https://doi.org/10.1021/je0255224
- Živković, E.M., Živković, N.V., Majstorović, D.M., Stanimirović, A.M., Kijevčanin, M.L.: Volumetric and transport properties of binary liquid mixtures with 1-ethyl-3-methylimidazolium ethyl sulfate as candidate solvents for regenerative flue gas desulfurization processes. J. Chem. Thermodyn. 119, 135–154 (2018). https://doi.org/10.1016/j.jct.2017.12.023
- Francesconi, R., Bigi, A., Rubini, K., Comelli, F.: Molar heat capacities, densities, viscosities, and refractive indices of poly(ethylene glycols) + 2-methyltetrahydrofuran at (293.15, 303.15, and 313.15) K. J. Chem. Eng. Data. 52(5), 2020–5 (2007). https://doi.org/10.1021/je7003066
- Yasmin, M., Gupta, M.: Density, viscosity, velocity and refractive index of binary mixtures of poly(ethylene glycol) 200 with ethanolamine, m-cresol and aniline at 298.15 K. J. Solution Chem. 40(8), 1458–72 (2011). https://doi.org/10.1007/s10953-011-9731-1
- 38. Awwad, A.M., Al-Dujaili, A.H., Salman, H.E.: Relative permittivities, densities, and refractive indices of the binary mixtures of sulfolane with ethylene glycol, diethylene glycol, and poly(ethylene glycol) at 303.15 K. J. Chem. Eng. Data. 47(3), 421–4 (2002). https://doi.org/10.1021/je010259c
- Wu, T.-Y., Chen, B.-K., Hao, L., Lin, K.-F., Sun, I.W.: Thermophysical properties of a room temperature ionic liquid (1-methyl-3-pentyl-imidazolium hexafluorophosphate) with poly(ethylene glycol). J. Taiwan Inst. Chem. Engin. 42(6), 914–921 (2011). https://doi.org/10.1016/j.jtice.2011.04.006
- Hemmat, M., Moosavi, M., Dehghan, M., Mousavi, E., Rostami, A.A.: Thermodynamic, transport and optical properties of formamide + 1,2-ethanediol, 1,3-propanediol and poly (ethylene glycol) 200 binary liquid mixtures. J. Mol. Liq. 233, 222–235 (2017). https://doi.org/10.1016/j.molliq. 2017.03.008
- Moosavi, M., Omrani, A., Ali Rostami, A., Motahari, A.: Isobaric, isothermal theoretical investigation and examination of different prediction equations on some physicochemical properties in PEG liquid polymer system. J. Chem. Thermodyn. 68, 205–215 (2014). https://doi.org/10.1016/j.jct.2013.09.006
- 42. Wu, T.-Y., Chen, B.-K., Hao, L., Lin, Y.-C., Wang, H.P., Kuo, C.-W., et al.: Physicochemical properties of glycine-based ionic liquid [QuatGly-OEt][EtOSO₃] (2-Ethoxy-1-ethyl-1,1-dimethyl-2-oxoethanaminium ethyl sulfate) and its binary mixtures with poly(ethylene glycol) (MW = 200) at various temperatures. Int. J. Mol. Sci. 12, 8750–8772 (2011). https://doi.org/10.3390/ijms12128750
- 43. Chaudhary, N., Nain, A.K.: Densities, speeds of sound, refractive indices, excess and partial molar properties of polyethylene glycol 200 + methyl acrylate or ethyl acrylate or *n*-butyl acrylate binary mixtures at temperatures from 293.15 to 318.15 K. J. Mol. Liq. 271, 501–13 (2018). https://doi.org/10.1016/j.molliq.2018.09.020
- Sengwa, R.J., Dhatarwal, P., Choudhary, S.: Static permittivities, viscosities, refractive indices and electrical conductivities of the binary mixtures of acetonitrile with poly(ethylene glycol)-200 at temperatures 288.15–318.15 K. J. Mol. Liq. 271, 128–35 (2018). https://doi.org/10.1016/j.molliq. 2018.08.137



- Sengwa, R.J., Choudhary, S., Dhatarwal, P.: Dielectric and electrical behaviour over the static permittivity frequency regime, the refractive indices and viscosities of PC-PEG binary mixtures. J. Mol. Liq. 252, 339–350 (2018). https://doi.org/10.1016/j.molliq.2017.12.139
- 46. Yasmin, M., Gupta, M., Shukla, J.P.: Experimental and computational study on viscosity and optical dielectric constant of solutions of poly (ethylene glycol) 200. J. Mol. Liq. **160**(1), 22–29 (2011). https://doi.org/10.1016/j.molliq.2011.02.005
- Branco, A.S.H., Calado, M.S., Fareleira, J.M.N.A., Visak, Z.P., Canongia Lopes, J.N.: Refraction index and molar refraction in ionic liquid/PEG200 solutions. J. Solution Chem. 44(3–4), 431–439 (2015). https://doi.org/10.1007/s10953-014-0277-x
- 48. Sengwa, R.J., Sankhla, S., Sharma, S.: Refractometric study of polymers and their blends in solution. Indian J. Chem. Sect. A. **46A**(9), 1419–22 (2007)
- 49. Van Geet, A.L.: Calibration of the methanol and glycol nuclear magnetic resonance thermometers with a static thermister probe. Anal. Chem. 40, 2227–2229 (1968)
- Jerschow, A., Müller, N.: 3D diffusion-ordered TOCSY for slowly diffusing molecules. J. Magn. Reson. A. 123, 222–225 (1996)
- Jerschow, A., Müller, N.: Suppression of convection artifacts in stimulated-echo diffusion experiments: Double-stimulated-echo experiments. J. Magn. Reson. 125, 372–375 (1997)
- 52. Nicolay, K., Braun, K.P.J., de Graaf, R.A., Dijkhuizen, R.M., Kruiskamp, M.J.: Diffusion NMR spectroscopy, NMR Biomed. 14, 94–111 (2001)
- Hoffmann, M.M., Bothe, S., Gutmann, T., Buntkowsky, G.: Combining freezing point depression and self-diffusion data for characterizing aggregation. J. Phys. Chem. B. 122(18), 4913–4921 (2018). https://doi.org/10.1021/acs.jpcb.8b03456
- Tammann, G., Hesse, W.: Die Abhängigkeit der Viscosität von der Temperatur bie unterkühlten Flüssigkeiten. Z. Anorg. Allg. Chem. 156(1), 245–257 (1926). https://doi.org/10.1002/zaac.19261 560121
- Garland, C.W., Nibler, J.W., Shoemaker, D.P.: Experiments in Physical Chemistry, 8th edn. McGraw-Hill, New York (2009)
- Zuccaccia, D., Maccioni, A.: An accurate methodology to identify the level of aggregation in solution by PGSE NMR measurements: The case of half-sandwich diamino ruthenium(II) salts. Organometallics 24(14), 3476–3486 (2005)
- Hayamizu, K., Tsuzuki, S., Seki, S., Fujii, K., Suenaga, M., Umebayashi, Y.: Studies on the translational and rotational motions of ionic liquids composed of *N*-methyl-*N*-propyl-pyrrolidinium (P13) cation and bis(trifluoromethanesulfonyl)amide and bis(fluorosulfonyl)amide anions and their binary systems including lithium salts. J. Chem. Phys. 133(19), 194505 (2010). https://doi.org/10.1063/1. 3505307
- 58. Macchioni, A., Ciancaleoni, G., Zuccaccia, C., Zuccaccia, D.: Determining accurate molecular sizes in solution through NMR diffusion spectroscopy. Chem. Soc. Rev. 37, 479–489 (2008)
- Chen, H.-C., Chen, S.-H.: Diffusion of crown ethers in alcohols. J. Phys. Chem. 88, 5118–5121 (1984)
- 60. Gierer, A., Wirtz, K.: Molecular theory of microfriction. Z. Naturforsch. A. 8, 532-538 (1953)
- 61. Van der Bondi, A.: Waals volumes and radii. J. Phys. Chem. 68, 441–451 (1964)
- Edward, J.T.: Molecular volumes and the Stokes–Einstein equation. J. Chem. Educ. 47, 261–270 (1970)
- Hoffmann, M.M., Too, M.D., Paddock, N.A., Horstmann, R., Kloth, S., Vogel, M., et al.: On the behavior of the ethylene glycol components of polydisperse polyethylene glycol PEG200. J. Phys. Chem. B. 127, 1178–1196 (2023)
- Chang, I., Fujara, F., Geil, B., Heuberger, G., Mangel, T., Sillescu, H.: Translational and rotational molecular motion in supercooled liquids studied by NMR and forced Rayleigh scattering. J. Non-Cryst. Solids. 172–174, 248–255 (1994)
- Cicerone, M.T., Ediger, M.D.: Enhanced translation of probe molecules in supercooled o-terphenyl: Signature of spatially heterogeneous dynamics? J. Chem. Phys. 104, 7210–7218 (1996)
- Hoffmann, M.M., Bothe, S., Gutmann, T., Buntkowsky, G.: Unusual local molecular motions in the solid state detected by dynamic nuclear polarization enhanced NMR spectroscopy. J. Phys. Chem. C. 121(41), 22948–22957 (2017). https://doi.org/10.1021/acs.jpcc.7b07965
- Hoffmann, M.M., Too, M.D., Vogel, M., Gutmann, T., Buntkowsky, G.: Breakdown of the Stokes-Einstein equation for solutions of water in oil reverse micelles. J. Phys. Chem. B. 124(41), 9115– 9125 (2020). https://doi.org/10.1021/acs.jpcb.0c06124
- Turton, D.A., Wynne, K.: Stokes-Einstein-Debye failure in molecular orientational diffusion: exception or rule? J. Phys. Chem. B. 118(17), 4600-4604 (2014). https://doi.org/10.1021/jp501 2457



- Yamaguchi, T.: Decoupling between solvent viscosity and diffusion of a small solute induced by self-motion. J Phys Chem Lett. 12(32), 7696–7700 (2021). https://doi.org/10.1021/acs.jpclett. 1c02219
- 70. Kumar, A., Singh, T., Gardas, R.L., Coutinho, Jo.A.P.: Non-ideal behaviour of a room temperature ionic liquid in an alkoxyethanol or poly ethers at *T*=(298.15 to 318.15)K. J. Chem. Thermodyn. **40**(1), 32–9 (2008). https://doi.org/10.1016/j.jct.2007.06.002

Publisher's Note Springer Nature remains neutral with regard to jurisdictional claims in published maps and institutional affiliations.

Springer Nature or its licensor (e.g. a society or other partner) holds exclusive rights to this article under a publishing agreement with the author(s) or other rightsholder(s); author self-archiving of the accepted manuscript version of this article is solely governed by the terms of such publishing agreement and applicable law.

Authors and Affiliations

Markus M. Hoffmann¹ · Nathaniel P. Randall¹ · Miray H. Apak¹ · Nathaniel A. Paddock¹ · Torsten Gutmann² · Gerd Buntkowsky²

- Markus M. Hoffmann mhoffman@brockport.edu
- ☐ Gerd Buntkowsky gerd.buntkowsky@chemie.tu-darmstadt.de
- Department of Chemistry and Biochemistry, State University of New York Brockport, NY 14420, USA
- Institute of Physical Chemistry, Technical University Darmstadt, Alarich-Weiss-Straße 8, 64287 Darmstadt, Germany

